Numerical investigation of hinged connector performance in modular floating platforms

To cite this article: S. Panda *et al* 2025 *IOP Conf. Ser.: Earth Environ. Sci.* **1552** 012021

IOP Conf. Series: Earth and Environmental Science **1552** (2025) 012021 doi:10.1088/1755-1315/1552/1/012021

Numerical investigation of hinged connector performance in modular floating platforms

PANDA, S.[1], MONTEIRO, K.[2], STAVRIDOU, N.[3], HILO, A.[4], GKANTOU, M.[5] ,VELJKOVIC, M.[6]

[1,*] Atlantic Technological University, Ireland;
[2]University of Coimbra, Portugal;
[3]Aristotle University of Thessaloniki, Greece;
[4]University of A Coruna, Spain;
[5]Liverpool John Moores University, UK;
[6]TU Delft, Netherlands

*E-mail: saleema.panda@atu.ie

Abstract. The conceptual design of modular floating energy islands involves the integration of renewable energy sources, such as wind turbines and solar panels, onto floating structures. These modular systems offer advantages, such as minimal environmental impact and adaptability to different coastal and environmental conditions. This study focuses on the design of connections between the floating modules. Hinged joints are identified as a promising connector type due to their balance of flexibility and strength. Advanced numerical simulations are employed to assess the hydrodynamic forces and structural responses of floating platforms. A hinged connection model is numerically developed and the simulated performance shows good agreement with published results. Subsequently, three different connection configurations are evaluated, and their responses are discussed. Among these, a three-hinge connection system is found to be efficient, minimising relative displacement between the platforms.

1. Introduction

Increasing global energy demands along with the need for mitigating the greenhouse effect consequences, make imperative the turn towards renewable energy production; which is documented in the revised European Commission directive setting for 2030 the target of a minimum 42.5% of total energy production coming from renewables [1]. In the last 25 years, the expansion of renewable energy production installations has been massive with renewables constituting 18% of the global energy production in 2000 and in 2024 the percentage being almost double, reaching 33.5% [2]. As offshore floating energy platforms move toward large-scale deployment and multi-modular configurations, the loads on connectors between the modules and their operational behaviour become critical factors in the design process. Due to the high stresses that pass through the connectors, they should be carefully designed, with special consideration to their dynamic responses [3,4].

Rigid joints, hinged joints, and flexible joints are the three broad categories into which connectors can be divided [2]. Model testing has shown that under severe sea conditions, stiff joint connectors are subjected to significant design loads. Furthermore, the structure of the flexible joint connector is comparatively more challenging. Consequently, hinged joint connectors can serve as an effective alternative to overcome the limitations of other types of connectors [5]. his study contributes to a deeper understanding of hinged joint connections by investigating the performance of hinged connectors through advanced numerical simulations, evaluating both hydrodynamic forces and the resulting structural response. Different geometries and configurations are studied with the aim of reducing the relative displacement between connected units, thus enhancing overall performance.

2. Research Methodology

2.1. Description of the model

A numerical model consisting of two floating bodies (F1, F2) connected with a hinged joint is developed with DualSPHysics [6]. The floating bodies (platform) are of dimensions 1m×0.2m×0.15m, similar to the one used by Song et al. [7] for validation purposes. The wave conditions used in the simulation replicate those reported by Song et al. [7], characterized by a wave height of 0.03 m and a wave period of 1.16 s.

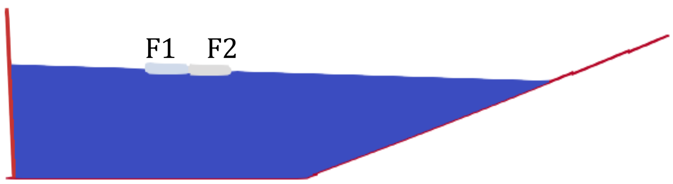

(a)

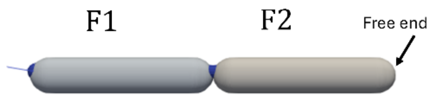

(b)

Figure 1. (a) Numerical model of two floating bodies (platforms) in wave tank (b) Hinged joint between the platforms

2.2. Theoretical basis of numerical modelling

The numerical model was developed using DualSPHysics, an open-source Smoothed Particle Hydrodynamics (SPH) solver jointly developed by the University of Vigo (Spain) and the University of Manchester (UK). DualSPHysics is specifically designed to address complex engineering problems using the SPH method, and it is capable of running on both central processing units (CPUs) and graphics processing units (GPUs). Given the superior computational power of GPUs over CPUs, and their relatively low cost, GPUs represent a cost-effective solution for accelerating SPH simulations. As such, DualSPHysics can be executed efficiently on personal computers equipped with GPU cards. In scenarios where high temporal and spatial resolution is required, particularly when dominant modes of fluid–structure interaction are not clearly defined, advanced numerical methods and high-performance computing capabilities become essential, especially for large-domain simulations.

The SPH approach computes hydrodynamic forces by solving differential-algebraic equations, while the motion of the floating bodies is updated iteratively using a symplectic time integration scheme. The SPH method is a mesh-free, Lagrangian approach that represents a continuum through a finite number of particles, each carrying physical properties such as mass,

density, velocity, and pressure. The governing equations are evaluated at the particle positions using a smoothing kernel function W, which enables interpolation over the domain.
A function $F(\boldsymbol{r})$ can be defined in r' as:

$$F(r) = \int F(r')W(r - r', h)dr' \quad (1)$$

where W is the kernel function, h is the smoothed length, and r'represents the position vector of the particle. A discrete approximation of the vector function F in Equation (1) at particle a is:

$$F(r_a) = \sum_b F(r_b)\frac{m_b}{\rho_b}W(r_a - r_b, h) \quad (2)$$

where b is summed over all the particles within the domain in which the smoothing length is defined, m_b is the mass of particle b, and r_b is the density of particle b. The performance of an SPH model is determined by the choice of the kernel function. A kernel function can be expressed in terms of the non-dimensional distance q, which is defined as $q = r/h$, where r is the distance of any given particle a to particle b.

The weight function plays a key role in SPH. Several conditions should be adopted, such as positive solution, integrated support, normalization, unilateral attenuation, and delta-function behaviour [8]. In our simulations, the following quantic kernel function developer in [9] was used:

$$W(r,h) = \alpha_D\left(1 - \frac{q}{2}\right)^4(2q + 1)0 \leq q \leq 2 \quad (3)$$

$$\alpha_D = \{\frac{7}{4\pi h^2}, in\ 2D\ \frac{21}{16\pi h^3}, in\ 3D \quad (4)$$

The SPH form of the continuity equation is:

$$\frac{d\rho_a}{dt} = \sum_b m_b V_{ab} \cdot \nabla_a W_{ab} \quad (5)$$

In DualSPHysics, the SPH fluid is weakly compressible. Then, the equation of state [10] can be written as:

$$P = b\left[\left(\frac{\rho}{\rho_0}\right)^\gamma - 1\right] \quad (6)$$

$$b = \frac{c_0^2\rho_0}{\gamma} \quad (7)$$

where γ = 7, ρ_0 is the reference density of 1000 kg/m3, and c_0 is the speed of sound at the reference density.

2.3. Development of the numerical model

The numerical model developed for this study and shown in Figure 1a uses the SPH method to calculate the wave forces. The tank is inclined on the left side (opposite to the wavemaker) to allow for wave absorption and natural dissipation like on a real coastline. Similar to the experimental model used for validation, in the present numerical model, one end of the first platform F1 is connected through the mooring cable, while the other end is connected through a hinged joint with the second platform F2. The other end of platform F2 is free, as shown in Figure 1b. The mooring cable is modelled using a lumped-mass mooring line model based on the finite element method, where the cable is discretized into a series of point masses connected by linear spring-damper elements. The mooring cable is coupled with the F1 platform using a 3-degree-of-freedom (surge, heave, and pitch) attachment that links the fairlead point to the platform.

The wavemaker in the model emulates the behaviour similar to the piston in the experimental environment to produce the desired waves. The forces on the floating bodies and the hinged connector due to the wave forces are calculated by solving differential-algebraic equations. The floating body positions are updated, and the steps are repeated for the next time step using a symplectic integrator. Based on the results of an initial sensitivity analysis, a smoothing length ratio of 1.1 and an artificial viscosity coefficient of 0.01 were identified as the most suitable parameters [11] for the model. This combination provided an optimal balance between numerical stability and physical accuracy, ensuring realistic fluid behaviour, while minimizing excessive damping effects that could distort fluid–structure interaction.

2.4. Validation of the numerical model

To assess the accuracy of the developed model, the numerically obtained longitudinal direction (Fx) is compared with the experimental values reported in [7], and the results are shown in Figure 2. The present result corresponding to the initial one-second duration is not shown in the graph due to initial noise in the numerical simulation. The peak forces occur at the same time in both cases, indicating good phase agreement. However, the simulated peak values are higher than those observed experimentally. This discrepancy is primarily attributed to the absence of damping in the numerical model, which leads to an overestimation of the dynamic response. In the numerical model using DualSPHysics, the hinged connector is represented as a massless, frictionless constraint with infinite stiffness, implemented as an ideal revolute. This idealization allows relative rotation between the two platforms about a fixed axis while eliminating any compliance, damping, or mass effects. In contrast, the experimental hinge consists of a physical connector assembly composed of five aluminium components, which inherently introduce mass, material damping, and finite stiffness into the system. Despite this, the overall force trend closely follows the experimental curve, demonstrating that the model captures the key dynamic behaviour of the system. The focus of this section is to evaluate the hydrodynamic forces acting on the platforms in Section 3.1 due to wave interaction, using the simplified hinged model. These force results will subsequently be used in the design optimization of the hinged connector in Section 3.2.

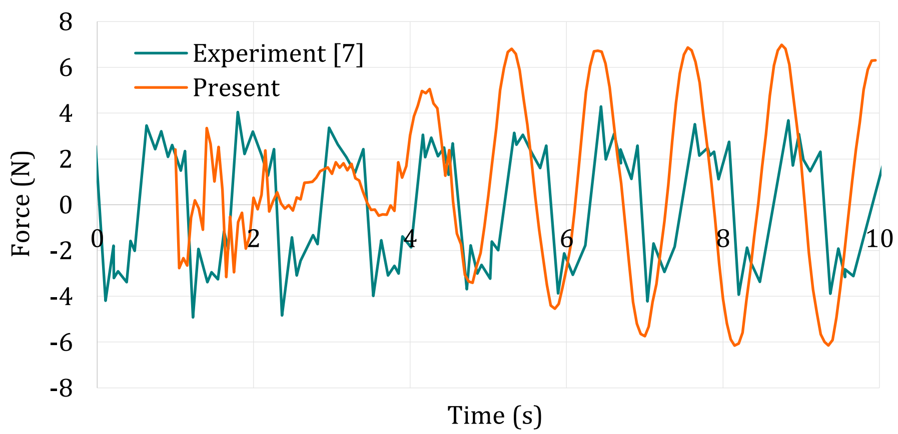

IOP Conf. Series: Earth and Environmental Science **1552** (2025) 012021 doi:10.1088/1755-1315/1552/1/012021

Figure 2. Comparison of longitudinal force at hinged connector with experimental results [7]

3. Results and Discussion

3.1. Forces and Displacements of Interconnected Floating Platforms

Having successfully validated the numerical models, a 1:50 scale model was adopted for further investigation and the conceptual design of the hinged connectors. Simulated wave conditions were specific to Portugal's coast (mean height 2.12 m, period 10.92 s) [12]. The Froude number [13] is used for scaling down the real model.

- Mean height for the scaled model = 2.12/*scale factor* = 0.0424 m
- Mean wave period for the scaled model = $10.92/\sqrt{scale\ factor}$ = 1.54 sec

The wave elevations used in this study over a 20-second period are shown in Figure 3. Forces and displacements in platforms F1 and F2 were analysed with the aim to optimise the hinged geometry and material distribution. In particular, the forces in both the platforms (F1, F2) due to the waves are presented in Figure 4. The longitudinal force arises due to the inertial effects of the moving floating body and hydrodynamic pressure acting on the surfaces. The displacement of the platforms is presented in Figure 5. Platform F2 shows more surge (dx) (see Figure 5a) due to the reaction to platform F1 and its own wave forces. Vertical forces in the platforms come mainly from buoyancy variations due to wave elevation changes, wave pressure distribution on the submerged surfaces, and inertia of the body mass in vertical acceleration. The heave (dz) (see Figure 5b) follows the wave shape but with less amplitude in platform F2 than in F1 due to constraints at the joint.

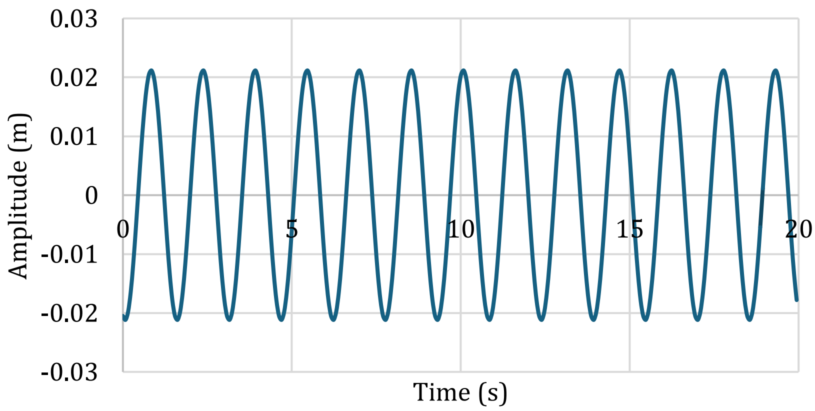

Figure 3. Wave amplitude versus time input for numerical simulation

3.2. Investigation of three hinged connection configurations

The model presented in Section 3.1 was also developed using finite element analysis in ABAQUS software [14], with the aim of investigating different hinged connection configurations. The initial step involved extracting displacement and force data from the numerical analysis using DualSPHysics and importing them into ABAQUS to enable validation and comparative analysis. The first connection configuration modelled was a simple hinge, consistent with the setup used in the DualSPHysics analysis. The dimensions of the connection (in mm) are shown in Figure 6a. The simulation in ABAQUS was limited to a single wave period due to computational cost. The resulting stress levels were found to be reasonably comparable to those obtained from the DualSPHysics model. The displacement results from the ABAQUS model also showed good agreement with those from the DualSPHysics simulations.

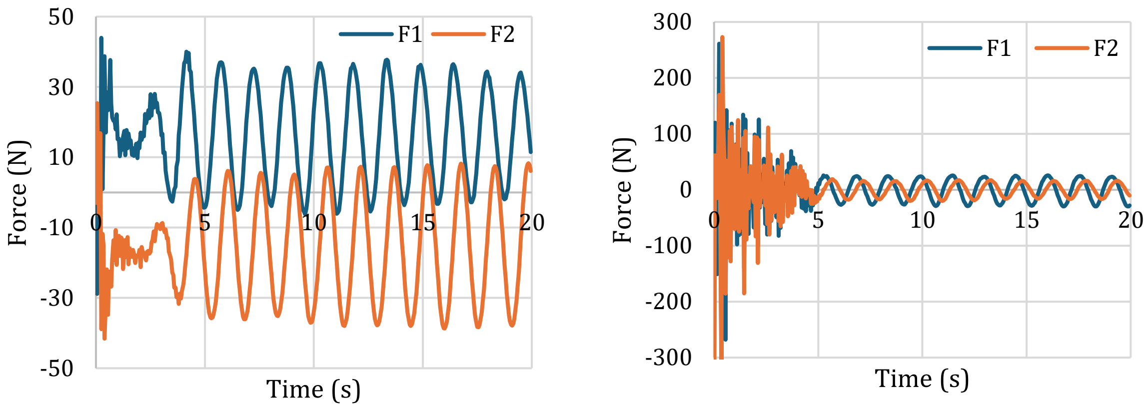

(a) Longitudinal force Fx (b) Vertical force Fz

Figure 4. Forces in platforms F1 and F2

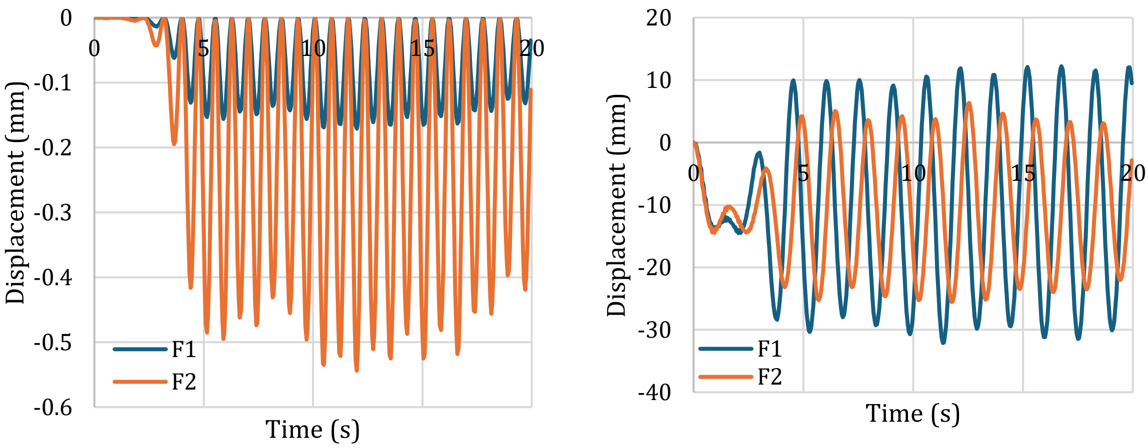

(a) Longitudinal displacement dx (b) Vertical displacement dz

Figure 5. Displacements in platforms F1 and F2

Following the comparison between ABAQUS model and DualSPHysics simulations, three hinged connection configurations (C1, C2, C3), shown in Figure 6, were modelled to analyse the resulting stresses and displacements, with a particular focus on vertical displacements. Compared to C1, connection C2 includes additional bars linking the hinge to the floating bodies. These bars have a square cross-section of 50 × 50 mm and a length of 140 mm. In C3, the three-hinged system was applied, and additional hinges were incorporated into the connection, linking each bar to the floating bodies. These additional hinges had the same dimensions as the original ones. The analysis examined how vertical displacement from one floating body (F1) was transferred to the other (F2) through the connection. The hinge and pin dimensions are presented in Figure 6a.

IOP Conf. Series: Earth and Environmental Science **1552** (2025) 012021 doi:10.1088/1755-1315/1552/1/012021

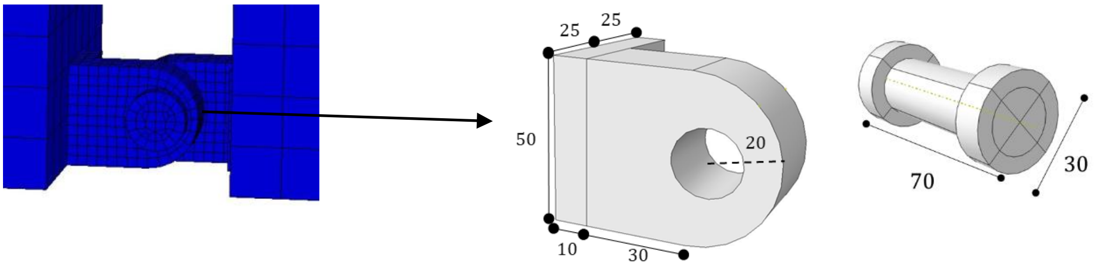

(a) Simple hinge (C1)

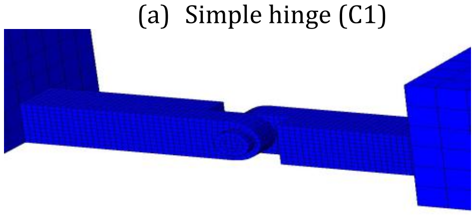

(b) Hinge with bars (C2)

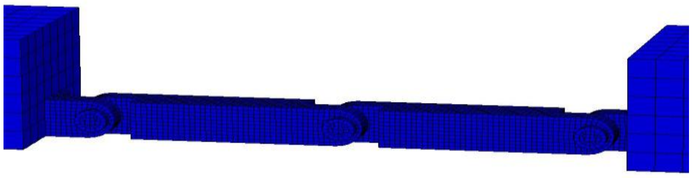

(c) Three hinges system (C3)

Figure 6. Examined hinged connection configuration types

The results for all connection configurations are presented in Figure 7 for one wave cycle, where the relative displacement between F1 and F2 due to wave action can be assessed. For the simple connection (C1), Platform 1 (F1) transferred more than 60% of its vertical displacement to Platform 2 (F2). In connection C2, the addition of bars to the hinged system slightly reduced the vertical displacement transferred from F1 to F2. In the third connection (C3), almost no vertical displacement was transferred from F1 to F2, as the connection effectively absorbed a significant portion of F1's vertical motion. The deformed shapes are shown in Figure 8, illustrating the ability of the three-hinge connection to dissipate a considerable component of the vertical displacement between the two platforms. The von Mises stress (MPa) in the hinge and pin area of all three configurations is presented in Figure 9. It can be observed that case C3 has significantly lower stress in the hinge and pin area than the other two types, which shows the successful use of the hinge in the offshore structures.

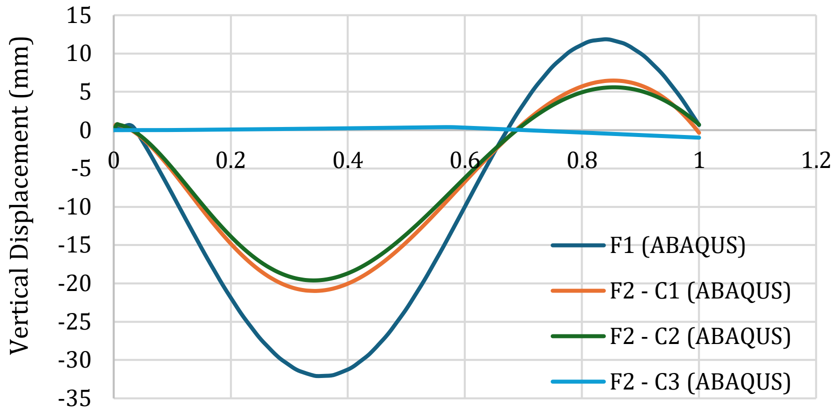

Figure 7. Vertical displacements of three examined hinged configuration types

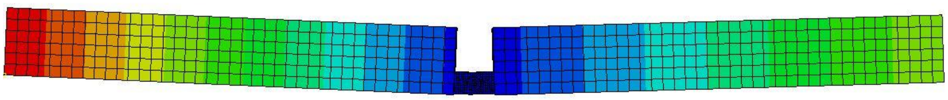

(a) Simple hinge (C1)

(b) Hinge with bars (C2)

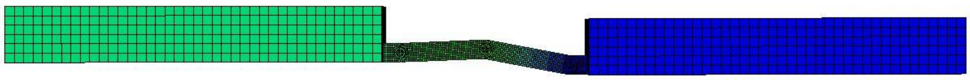

(c) Three hinges system (C3)

Figure 8. Deflected shapes of three examined hinged configuration types

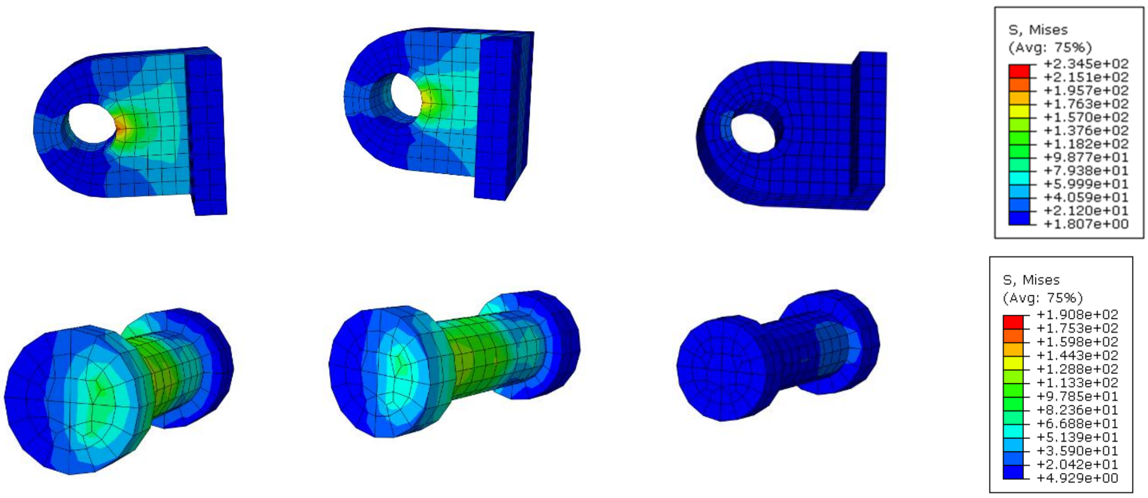

(a) case C1 (b) case C2 (c) case C3

Figure 9. Stress (MPa) Distribution for the Three Examined Hinged Configuration Types and Their Corresponding Pins

4. Conclusions

This study demonstrated the feasibility and potential advantages of hinged connections in modular floating islands for renewable energy generation. By optimising the connector design through numerical study using Abaqus and Dual-SPH, the structural performance and practicality of these floating systems can be assessed and enhanced. Three connector designs featuring different hinged connection configurations were modelled and compared. The findings of this research, together with recent industrial advancements by Stiesdal in offshore connections [15], support the viability of hinged connections as a sustainable and adaptable solution for modular floating islands [16, 17] in offshore renewable energy infrastructure.

Acknowledgments

The authors would like to acknowledge COST Action 20109 MODENERLANDS because it gave the opportunity to researchers from various countries to fruitfully collaborate.

References

[1] European Commission. 2014, Communication from the commission to the European parliament, the council, the European economic and social committee and the committee of the regions. A policy framework for climate and energy in the period from 2020 to 2030 Available online at https://eur-lex.europa.eu/
[2] IEA. (2023). Renewables 2023 - Analysis. https://www.iea.org/reports/renewables-2023
[3] Suzuki, H. Safety target of very large floating structure used as a floating airport. Mar. Struct. 2001, 14, 103–113.Shi, Q.; Xu, D.; Zhang, H. Design of a Flexible-Base Hinged Connector for Very Large Floating Structures. In Proceedings of the ASME 2018 37th International Conference on Ocean, Offshore and Arctic Engineering, Madrid, Spain, 17–22 June 2018.
[4] Suzuki, H.; Harada, H.; Natsume, T.; Maeda, K.; Iijima, K.; Hayashi, T. Technical Challenge on VLFS in Japan After Mega-Float Project. In Proceedings of the ASME 2017 36th International Conference on Ocean, Offshore and Arctic Engineering, Trondheim, Norway, 25–30 June 2017; p. V009T12A013.
[5] Shi, Q.; Xu, D.; Zhang, H. Design of a Flexible-Base Hinged Connector for Very Large Floating Structures. In Proceedings of the ASME 2018 37th International Conference on Ocean, Offshore and Arctic Engineering, Madrid, Spain, 17–22 June 2018.
[6] Crespo, A. J. C., Domínguez, J. M., Rogers, B. D., Gómez-Gesteira, M., Longshaw, S., Canelas, R., Vacondio, R., Barreiro, A., & García-Feal, O. (2015). DualSPHysics: Open-source parallel CFD solver based on Smoothed Particle Hydrodynamics (SPH). Computer Physics Communications, 187, 204–216. https://doi.org/10.1016/j.cpc.2014.10.004
[7] Song, X., Liu, W. and Wu, H., 2023. Investigation on Load Characteristics of Hinged Connector for a Large Floating Structure Model under Wave Actions. Journal of Marine Science and Engineering, 11(4), p.786.
[8] Liu, G.R. and Liu, M.B., 2003. Smoothed particle hydrodynamics: a meshfree particle method. World scientific.
[9] Wendland, H., 1995. Piecewise polynomial, positive definite and compactly supported radial functions of minimal degree. Advances in computational Mathematics, 4, pp.389-396.
[10] Zhang, F., Zhang, L., Xie, Y., Wang, Z. and Shang, S., 2021. Smoothed particle hydrodynamics simulation of a agriculture platform under waves. Water, 13(20), p.2847.
[11] Green, M.D. and Peiró, J., 2018. Long duration SPH simulations of sloshing in tanks with a low fill ratio and high stretching. Computers & fluids, 174, pp.179-199.
[12] Silva, K., Abreu, T. and Oliveira, T.C., 2022. Inter-and intra-annual variability of wave energy in Northern mainland Portugal: Application to the HiWave-5 project. Energy Reports, 8, pp.6411-6422.
[13] Hughes, Steven A, 1993. Physical Models and Laboratory Techniques in Coastal Engineering. Singapore, World Scientific.
[14] Dassault Systèmes, 2024. Abaqus 2024 User Guide. Providence, RI: Dassault Systèmes.
[15] The vital role of floating wind, Stiesdal. https://www.stiesdal.com/offshore/the-vital-role-of-floating-wind Accessed 16.05.2025

[16] Marino, E., Gkantou, M., Malekjafarian, A., Bali, S., Baniotopoulos, C., van Beeck, J., Borg, R.P., Bruschi, N., Cardiff, P., Chatzi, E. and Čudina, I., 2025. Offshore renewable energies: exploring floating modular energy islands—materials, construction technologies, and life cycle assessment. Journal of Ocean Engineering and Marine Energy, pp.1-26.
[17] Marino, E., Gkantou, M., Malekjafarian, A., Bali, S., Baniotopoulos, C., van Beeck, J., Borg, R.P., Bruschi, N., Cardiff, P., Chatzi, E. and Čudina, I. (2024) Offshore renewable energies: A review towards Floating Modular Energy Islands—Monitoring, Loads, Modelling and Control. Ocean engineering, 313, p.119251.